Multilevel Microfluidics via Single-Exposure Photolithography

Michael W. Toepke and Paul J. A. Kenis*

*Department of Chemical & Biomolecular Engineering, University of Illinois at Urbana-Champaign,
600 South Mathews Avenue, Urbana, Illinois 61801*

Received February 1, 2005; E-mail: kenis@uiuc.edu

The present work demonstrates a new technique that can be used to form multilevel features in SU-8 photoresist using a single lithography step, thereby minimizing or eliminating multistep protocols and alignment issues. The method utilizes the spatial dependence of diffracted light intensity to selectively overexpose certain masked regions of photoresist. The technique requires only a collimated UV light source and allows for a range of feature heights to be integrated simultaneously within a channel structure. Multilevel features have previously been used to enhance the performance and/or increase the capabilities of a variety of microfluidic devices. Staggered herringbone patterns have been integrated into microfluidic channels to promote chaotic mixing.[1] Ridge structures running between two phase liquid streams have been used to stabilize the liquid−liquid interfaces.[2] Multilevel features within a channel have also served as weirs to trap functionalized microbeads.[3] Relief features can also be added to microfluidic channels to increase surface area-to-volume ratios, which is useful for applications ranging from heterogeneous catalysis to heat transfer.

Solid-object printing,[4] laser machining,[5] stereolithography,[6] reaction−diffusion,[7] and multilayer processes[1,8] are among the methods that have been used to fabricate microfluidic channels with 3D structures, all of which require expensive equipment or extra processing steps. Alternatively, gray-tone masks have been used to form multilevel features in positive resists using a single exposure,[9,10] but many applications require higher aspect ratios than can be obtained in positive resists. SU-8 and other negative photoresists are commonly used when higher aspect ratios are required; however, gray-tone masks cannot be used with negative resists in traditional exposure systems because cross-linking is not selectively initiated at the surface of the substrate, which is necessary to achieve adhesion of the resist to the surface. Gray scale masks have been employed to fabricate multilevel features from SU-8 resist by exposing from the bottom of a transparent substrate,[11] but the method is not suitable when silicon or other opaque substrates are required. In addition, high-resolution gray scale masks are typically costly.

It has long been known that overexposure during photolithographic patterning leads to a loss in feature fidelity when the cumulative exposure of masked regions exceeds the energy dosage threshold at which cross-linking begins (E_T).[12] Overexposure is generally not a problem during routine processing of negative resists due to oxygen quenching of photoinitiated radicals,[13] the limited diffusion of radical species in dry photoresist, and the exponential decay of diffracted light. The intensity of diffracted light beneath a mask feature is related in a nonlinear manner to the location with respect to the mask edges.[14] A more detailed discussion regarding the relationship between intensity of diffracted light and location relative to an obstruction is presented in the Supporting Information. The present work uses variations in mask feature size to control the degree of superposition of diffracted light beneath mask elements and, hence, the degree of overexposure that occurs.

Figure 1 demonstrates the ability to selectively overexpose resist by controlling the degree of superposition of diffracted light using different mask feature sizes. Figure 1a is a schematic of the configuration used to pattern the photoresist with features of different heights in a single photolithographic exposure. The pattern was formed using a single transparency mask with a series of 100-μm open lines separated by a sequence of masking lines that increased in width in 5-μm increments. The mask was used to expose a 250-μm-thick layer of SU-8 on a silicon wafer to create a master with features of varying heights. A PDMS replica of this photoresist master is shown in Figure 1b, and the mask feature and replica feature sizes for each of the structures shown is provided in Table 1. The nonlinear response in replica feature size relative to mask feature size results from the degree of superposition of diffracted light from the two sides of the masking lines. The diffracted light intensity decays in an exponential manner beneath the masking feature, and thus the degree of superposition is much greater for smaller mask features and rapidly decays as the mask feature size increases. The nonlinear nature of this method allows users to control aspect ratios by making small adjustments in mask feature size.

The degree of overexposure is also determined by the amount of UV light that is incident on the mask. Figure 2a,b shows two PDMS replicas that were made from 178-μm-thick resists and a transparency mask consisting of three open lines separated by two masking lines. Figure 2a shows a PDMS replica made from a resist that was exposed to an incident dosage of 1.5 J/cm^2, approximately 150% more than the dosage recommended by the manufacturer. The replica shows that the mask pattern was transferred to the resist with good fidelity. Figure 2b shows a PDMS replica made from a resist treated with an incident dosage of 3 J/cm^2. The sidewalls are still vertical because there was no superposition of light beneath the mask to increase the total diffraction intensity to E_T. The tapered and truncated features between the three channels are evidence that E_T has been exceeded in the masked regions as a result of superposition of light. Further increasing the incident dosage leads to a continual decrease in feature size until the features eventually disappear. Hence, it is possible to obtain feature heights ranging from the thickness of the resist to no feature at all; however, it is not possible to obtain the entire spectrum of feature heights in a single device because of the nonlinear response discussed earlier. The number of feature heights that can be obtained in a device depends on the resolution of the mask and the size of features that are desired. The minimal spacing between individual mask features needed to achieve multilevel patterns depends largely on the thickness of the film being patterned, with thicker resists requiring more spacing between mask features. Separating mask features by 25 μm is generally sufficient for films up to 250-μm thick.
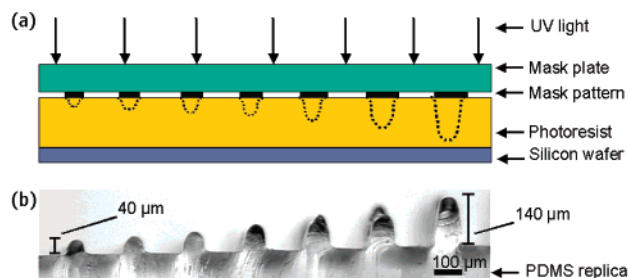
Figure 1. (a) Schematic diagram showing the formation of the master mold in photoresist. The mask contains 100-μm open lines separated by dark regions of various widths. (b) Optical micrograph of a PDMS replica of the master photoresist patterned with photolithography.

Table 1. Dimensions and Aspect Ratios of Resulting Features for Different Mask-Feature Sizes

mask (μm)	60	65	70	75	80	85	90
feature (μm)	40	50	62	78	98	118	140
aspect ratio	0.67	0.77	0.89	1.04	1.23	1.39	1.56
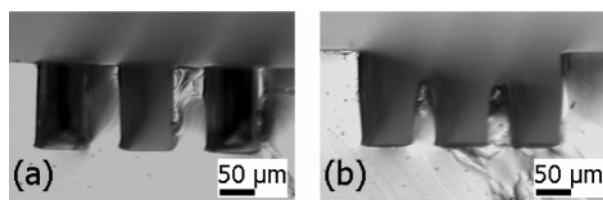
Figure 2. Cross sections of a PDMS replica made from a 178-μm-thick master after being exposed to (a) 1.5 J/cm^2 and (b) 3 J/cm^2 of incident light. Note that the sidewalls of the channel remain straight.
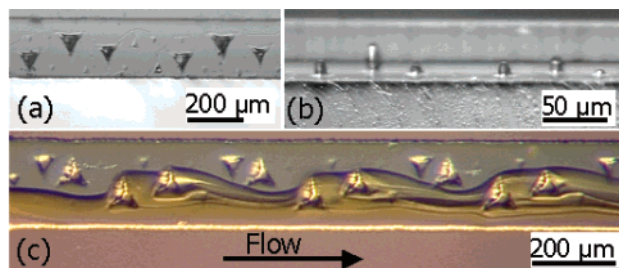
Figure 3. (a) Top view and (b) perspective side view along the direction of flow of a microfluidic channel with 3D triangle structures. (c) Top view of the initial ~2 mm of the same 2-cm-long channel with a blue and a yellow stream being mixed at a flow rate of 25 mL/hr.

To demonstrate the usefulness of the technique, a straight 2-cm-long, 200-μm-wide, and 57-μm-high channel was fabricated with integrated 3D features: a series of triangular pyramids of various heights (Figure 3a,b) obtained in a single photolithographic exposure using a single mask with differently sized triangular mask features. The slanted edges of the pyramids were expected to add a degree of asymmetry to the channel to aid in chaotic advection. Figure 3c shows blue and yellow aqueous streams being mixed in the initial portion (~2 mm) of the channel at a flow rate of 25 mL/hr. The interface between the two dyed streams undergoes a transition from a well-defined liquid−liquid interface, characteristic of laminar flow within featureless microfluidic channels, to a significantly perturbed liquid−liquid interface as a result of the pyramid structures within the channel.

The degree of mixing within the reactor was quantified by performing an acid−base reaction and comparing the amide yield to the yield obtained from a channel without features. A detailed description of the experiment is reported in the Supporting Information. Briefly, solutions of 5 mM phenylalanine methylester

and naproxen acid chloride (diffusivities of ~10^{-9} m^2/s) were each fed to the reactor at a rate of 15 mL/hr, resulting in a Reynolds number of 75. The reactor exit was formed by cutting off the channel at an alignment mark; the open end of the reactor was submerged in 5 mL of DI water to quench the reaction immediately after exiting the device. A total of 1 mL of reaction solution was collected and extracted from the aqueous solution using 2 mL of ethyl acetate. Large partition coefficients assured that the reagents and product were extracted into the ethyl acetate. The concentration of the respective components in the extract was determined by gas chromatography with the use of an internal standard. Three replicates of each sample were prepared, and the mean of these values, along with the standard deviations, are reported here. The yield from the reactor containing 3D features was 98% based on the naproxen acid chloride starting material with a standard deviation of 2%, which was statistically identical to the outcome of a control experiment. In contrast, the reactor with no features showed a yield of only 28% with a standard deviation of 5%, indicating that diffusion alone was unable to yield a completely mixed sample over the length of the channel. This marked increase in reaction yield observed in the channel with 3D features demonstrates the dramatic improvement that can be achieved by using multilevel features in microfluidic channels.

In sum, the new method presented here provides a simple means of obtaining 3D channel geometries using a transparency mask and any collimated UV light source without the need for extra alignment equipment and processing steps. Mixing structures, flow stabilization ridges, and separation weirs are just a few of the features that can be created using this new technique.

Supporting Information Available: Detailed descriptions of fabrication and experimental setup; brief theoretical discussion. This material is available free of charge via the Internet at http://pubs.acs.org.

References

(1) Stroock, A. D.; Dertinger, S. K. W.; Ajdari, A.; Mezit, I.; Stone, H. A.; Whitesides, G. M. *Science* **2002**, *295*, 647−651.

(2) Tokeshi, M.; Minagawa, T.; Uchiyama, K.; Hibara, A.; Sato, K.; Hisamoto, H.; Kitamori, T. *Anal. Chem.* **2002**, *74*, 1565−1571.

(3) Seong, G. H.; Zhan, W.; Crooks, R. M. *Anal. Chem.* **2002**, *74*, 3372−3377.

(4) McDonald, J. C.; Chabinyc, M. L.; Metallo, S. J.; Anderson, J. R.; Stroock, A. D.; Whitesides, G. M. *Anal. Chem.* **2002**, *74*, 1537−1545.

(5) Wolfe, D. B.; Ashcom, J. B.; Hwang, J. C.; Schaffer, C. B.; Mazur, E.; Whitesides, G. M. *Adv. Mater.* **2003**, *15*, 62−65.

(6) Mizukami, Y.; Rajniak, D.; Rajniak, A.; Nishimura, M. *Sens. Actuators, B* **2002**, *B81*, 202−209.

(7) Campbell, C. J.; Klajn, R.; Fialkowski, M.; Grzybowski, B. A. *Langmuir* **2005**, *21*, 418−423.

(8) Liu, R. H.; Stremler, M. A.; Sharp, K. V.; Olsen, M. G.; Santiago, J. G.; Adrian, R. J.; Aref, H.; Beebe, D. J. *J. Microelectromech. Syst.* **2000**, *9*, 190−197.

(9) Oppliger, Y.; Sixt, P.; Stauffer, J. M.; Mayor, J. M.; Regnault, P.; Voirin, G. *Microelectron. Eng.* **1994**, *23*, 449−454.

(10) Wagner, B.; Quenzer, H. J.; Henke, W.; Hoppe, W.; Pilz, W. *Sens. Actuators, A* **1995**, *A46*, 89−94.

(11) Afromowitz, M. A. *U. S. Pat. Appl. Publ.* **2002**, p 14.

(12) McGillis, D. A.; Fehrs, D. L. *IEEE Trans. Electron Devices* **1975**, *22*, 471−477.

(13) Shew, B.-Y.; Huang, T.-Y.; Liu, K.-P.; Chou, C.-P. *J. Micromech. Microeng.* **2004**, *14*, 410−414.

(14) Hecht, E. *Optics*, 3rd ed.; Addison-Wesley: Reading, MA, 1998; pp 476−505.

JA050660+